MODELLING AND SIMULATION OF A SUBSTRATE THERMOMECHANICAL BEHAVIOR DURING THE PLASMA SPRAYING

Kezrane Mohamed[1,2], Rebhi Redha[1,3]

[1]Department of Mechanical Engineering, Faculty of Technology, University of Medea, Medea (26000), Algeria

[2]Laboratory of Mechanics, Physics, and Mathematical modeling (LMP2M), University of Medea, Medea (26000), Algeria

[3]LERM-Renewable Energy and Materials Laboratory, University of Medea, Medea (26000), Algeria

Abstract

In our study, a 3D thermal plasma jet was simulated using the ANSYS-CFX code with two turbulence models and for different cases of effective powers. The analysis of the turbulent flow during the thermal jet using the RNG k-ε and SST k-ω models was also presented. The velocity and temperature profiles at the nozzle outlet were deduced from the literature and used as inlet boundary conditions. The results obtained from the two turbulence models show that the RNG k-ε model with different effective powers (790 W; 1050 W; 1350 W and 1780 W) is in good agreement with the experimental results. The RNG k-ε model gave results closer to the experiment than the results obtained from the SST k-ω model. It can also be concluded that when increasing the power supplied to the gas used, the temperature increases and it is maximum in the central axis. In the second step, the flow analyzed by the RNG k-ε model generated the initial conditions for the unsteady flow. Transient simulations for the 2D plasma jet are performed to obtain the velocity and temperature fields and also to obtain the temperature distribution in the substrate for the different time values. The transient simulations in the substrate for the different time values have also been studied. The results showed that the variation of the temperature of the plasma jet is always insignificant near the substrate for any value of time (flat curves) this says that the maximum of the temperatures obtained at the level of the substrate in the axial direction (Z axis) are maximum at the interface between the flow and the substrate (i.e. the contact surface at the centerline), and the maximum of the temperatures obtained at the substrate in the radial direction (y-axis) are maximum at the center of the substrate (i.e. x=0 and y= 0).

Keywords: *thermal plasma jet, turbulent flow, transient simulations, Substrate, ANSYS-CFX*

1. INTRODUCTION

The study of flows is a fundamental problem in fluid mechanics and heat transfer. The existing theoretical approach is flawed by the complexity of the phenomena and the equations. However, the blatant development of computer science has led to a revolution in numerical study methods which seek to obtain numerically approximate solutions for several types of flows and in particular the analysis of turbulent flow during thermal projection.

Thermal spraying is a family of surface treatment and coating formation processes on industrial parts [1]. The fields of application are very wide, from simple anti-wear and anti-corrosion processes (galvanizing for metal infrastructures), to higher technology applications such as in aircraft engines, in the field of medicine (prostheses), turbines gas, automotive, nuclear, electrical engineering, etc. The materials to be projected are generally in the form of powder, wire or rod and are subjected to a heat source [2]. These particles, if they have an adequate speed and temperature, impact the substrate and crash into it. As they spread and cool, they create a layer of material that adheres to the substrate. This makes it possible, by superimposing several layers of particles, to quickly create deposits of the order of a few hundred micrometers, deposits which bring about a change in the level of the interaction between the treated material and its environment. Plasma jet processes provide protection against wear, excessive temperature, chemical attack and environmental corrosion.

Coating manufacturing processes are varied and use different heat sources: plasma spraying, powder flame spraying, wire flame spraying, electric arc, supersonic flame spraying (HVOF) and detonation gun [3].

Plasma or "fourth state of matter" is an ionized medium, that is to say made up of a mixture of ions, electrons and neutral species, excited or not. This state is the normal state for more than 99% of the matter in the Universe [4]. Depending on the degree of ionization of the medium and its density, three types of plasma can be schematically distinguished:

- Fusion plasmas: these are totally ionized media. These plasmas are the most frequent in the Universe (star, sun); they are present during the explosion of a thermonuclear charge. Their characteristic temperature is a few tens of millions of degrees.
- Thermal or intermediate plasmas: weakly ionized media (20% maximum) and sufficiently dense for all the species present to have the same temperature, from 4000 to 50,000 K. These are the plasmas that are used for projection.
- "Cold" plasmas: weakly ionized and not very dense media so that only the electrons have a high temperature. This plasma is familiar to us, since it is present when we light a neon tube, in other words a fluorescent tube.

Blown arc spraying is commonly referred to as plasma spraying. Plasma projection consists of introducing solid particles into a jet of gas, the temperature of which generally reaches 12000 K and the speed of 1000-1500 m/s, and in which they are accelerated and melted before crashing into the part at coat called the substrate [5, 6]. The injection of the powder can be carried out outside the torch or in the terminal part of the anode itself, for certain applications. An electric discharge occurs between the anode and the cathode in the projection torch thanks to a direct current generator. The plasma gas is injected between the electrodes where the electric arc is produced. The gas undergoes molecular dissociation (for hydrogen) and/or partial ionization which produces strong expansion and relaxation of the plasma jet at the nozzle outlet.

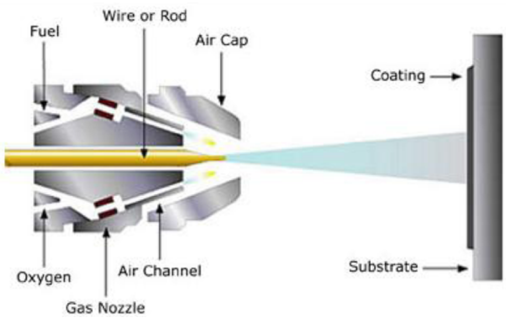

Fig. 1. Schematization of thermal spraying by plasma.

In our study we will be interested in the analysis of the three-dimensional turbulent flow for the analysis of the plasma jet for the stationary mode. The results obtained will be compared with those of the experiment and those found in the literature and under the same conditions in order to validate this model.

2. PROBLEM DEFINITION AND MATHEMATICAL FORMULATION

In this work, a 3D three-dimensional case of a thermal plasma jet was studied using argon as plasma gas for different powers, the plasma jet is assumed to be stable, incompressible, subsonic in local thermodynamic equilibrium and turbulent. Also, it is assumed that there is no segregation or chemical reactions in the gas phase. The Ansys CFX code, based on the finite volume method (FVM), was used to solve the conservation equations that govern the problem (Navier-Stokes and turbulence quantities) and this for all the turbulence models used in our study. The calculations are performed using the k-ε variant model. The pre-processor CFX code associated with Ansys 16.0 is used for the construction of the computational domain and the generation of the grid.

The geometry of the flow considered is shown in Figure 2. The dimensions of the calculation domain are respectively 100 mm and 50 mm for the length and the diameter of the cylinder. The z axis is aligned along the inlet stream, and the y axis is perpendicular to the x and z axis, the nozzle diameter is 3.0mm, the argon flow rate is 8 .4 liters/min.

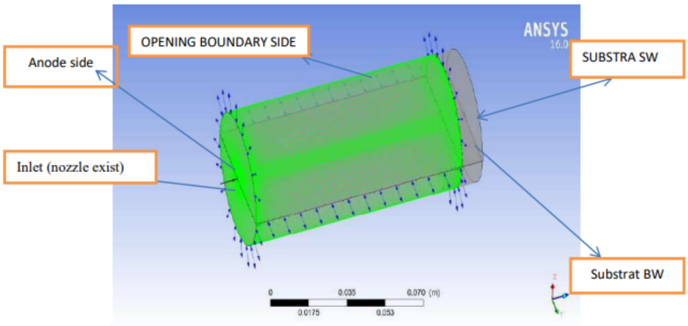

Fig. 2. 3D computational domain with CFX-Ansys (a thermal plasma spraying).

The modeling of the plasma jet is based on the resolution of the conservation equations of fluid mechanics and thermic for a monophasic multi-species mixture assimilated to a continuous medium.

Our model used the conservation equations for mass, species, momentum, energy and turbulence written in Cartesian coordinates in 3D, the conservation equations for mean turbulent flow were expressed as follows:

$$\underbrace{\frac{\partial}{\partial t}(\rho\phi)}_{A} + \underbrace{div(\rho\vec{v}\phi)}_{B} = \underbrace{div\left(\Gamma_\rho \overrightarrow{grad}\phi\right)}_{C} + \underbrace{S}_{S} \quad (1)$$

It should be noted that the notion "vectors" is attributed to the three components of the speed u, v and w while the notion "scalars" can designate the turbulent kinetic energy *k*, the dissipation energy, ε, the temperature, *T*, and the enthalpy, *h*.

The mass conservation equation which represents the instantaneous variation of mass is entirely linked to the transport of matter by the flow, the mass conservation equation is written:

$$\frac{\partial}{\partial t}(\phi) + div(\rho\vec{v}) = 0 \quad (2)$$

The momentum flow is related to the convective transport by the flow, pressure and gravity forces and viscous stresses, the momentum equation is written:

$$\frac{\partial}{\partial t}(\rho\vec{v}) + div(\rho\vec{v} \times \vec{v}) = -\overrightarrow{gradP} + f + div\vec{\tau} \quad (3)$$

The total energy equation is given by the following formula:

$$\frac{\partial(\rho h_{tot})}{\partial t} - \frac{\partial p}{\partial t} + div(\rho\vec{v}h_{tot}) = div(\lambda\nabla T) + div(\vec{v}\tau) + \vec{v}S_M + S_E \quad (4)$$

For first-order equations with two equations, we have seen in the previous paragraphs that to ensure the closure of the Reynolds equations, two additional equations must be added:

- The turbulent kinetic energy equation, k.
- The dissipation rate equation, ε.

$$\underbrace{\frac{\partial k}{\partial t}+\vec{u}_i\frac{\partial k}{\partial x_i}}=\underbrace{v_t\left(\frac{\partial \bar{u}_i}{\partial x_j}+\frac{\partial \bar{u}_j}{\partial x_j}\right)\frac{\partial \bar{u}_i}{\partial x_j}}+\frac{\partial}{\partial x_i}\left(v+\frac{v_t}{\sigma_k}\right)\frac{\partial k}{\partial x_j}-\varepsilon \qquad (5)$$

$$\frac{\partial \varepsilon}{\partial t}+\vec{u}_i\frac{\partial \varepsilon}{\partial x_i}=C_{1\varepsilon}\frac{\varepsilon}{k}\overline{u_i'u_j'}\frac{\partial \bar{u}_i}{\partial x_j}+\frac{\partial}{\partial x_i}\left[\left(v+\frac{v_t}{\sigma_\varepsilon}\right)\frac{\partial \varepsilon}{\partial x_j}\right]-C_{2\varepsilon}\frac{\varepsilon^2}{k} \qquad (6)$$

with $v_t = C_\mu \frac{k^2}{\varepsilon}$, $C\mu$ and σ_k are respectively the first and the second constant.

The values of constants resulting from a compromise between the families of flows constitute the standard values and which are presented as follows:

$$C_\mu = 0.09,\ C_{1\varepsilon} = 1.44,\ C_{2\varepsilon} = 1.92,\ \sigma_k = 1.0,\ \sigma_\varepsilon = 1.0$$

3. NUMERICAL SOLUTION

At the beginning, simulations are carried out for a flow without substrate, and then the substrate is introduced in the form of a disc having a thickness equal to 10 mm. A non-uniform Cartesian structured mesh in both Y and Z directions is used, and a circular structured mesh is used in the faces parallel to Z. Particular attention has been paid to the generation of the mesh, in particular to the processing near the walls. The computational domain is divided into six areas of non-uniform structured mesh, as shown in Figure 3. The location of the entry and exit boundaries and other boundaries with substrate are shown in Fig. 3. Additionally, Table. 1 presents the corresponding computational domain with 287874 elements for the computation with the substrate.

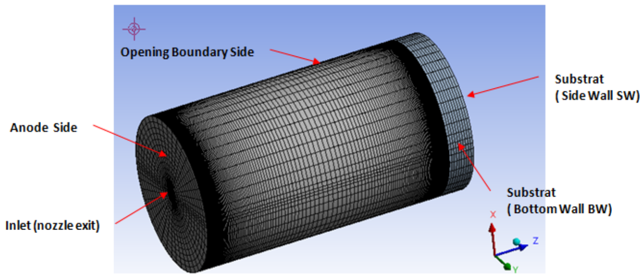

Fig. 3. 3D computational domain with meshing CFX - Ansys (a thermal plasma spraying) and 3D Boundaries designation with substrate.

Zone	Zone's name	Numbers of the nodes	Type of boundaries	values
B1	inlet	60	Temperature and velocity profiles	
B2	anode wall 1	60	Non slip wall	*T=500°K*
B3	outlet	150	Opening boundaries	
B4	interface	160	Conservative interface flux	
B5	substrate	160	Heat transfer coefficient and outside temperature	*Heat coef = 40* $W.m^{-2}.K^{-1}$
B6	substrate	40	Non slip wall	*T=300°K*

Table. 1. The numbers of the nodes in the different zones of the mesh zones.

Table. 1 presents the types of boundary conditions for the studied case, the denominations of zones of boundary conditions are mentioned in Fig. 3.

Snabre et al. [7] used formulas derived from the enthalpy equilibrium equation to obtain the values of Tmax and Umax at the nozzle inlet. where T_0 and U_0, Ua are calculated from Eqs. (7) to (10):

$$U_0 = U_a T_0 / T_a \tag{7}$$

$$U_a = 4Q/\pi D^2 \tag{8}$$

$$T_0 = \frac{-b\sqrt{(b^2-4ac)}}{2a} \tag{9}$$

where: $a = \frac{1}{2}\rho Q\left(\frac{U_a}{T_a}\right)^2$, $b = \rho Q C_P$ and $c = -\left(\frac{1}{2}\rho Q U_a^2 + \rho Q C_P T_a + P\right)$ (10)

By using the equations (7) to (10), we obtain the results mentioned in Table. 2 for the different power cases by aligning with the experimental data of Snabre et al. [7].

Cases	Power (W)	T_0 (K)	U_0(m/s)
Case a	790	6614,98	436,72
Case b	1050	8625,17	569,43
Case c	1300	10528,70	698,1
Case d	1780	14107,34	931,36

Table. 2. Maximum values of temperatures and velocities for different cases

The profiles of the turbulent kinetic energy k and the dissipation energy ε at the entrance are given respectively by the following expressions [8]:

$$K = 0.5 \times I_t \times V_z^2 \tag{11}$$

$$\varepsilon(r) = C_\mu \times K^2(r)/L_m \tag{12}$$

Also, the boundary conditions relating to the volume fractions of argon and air are presented in Table. 3.

	Inlet	Outlet	Opening side
% Air	0	100	100
% Argon	100	0	0

Table. 3. The volume fractions for air and argon for different boundaries.

The 'Opening' condition is defined so that the relative pressure is zero and the direction of flow is perpendicular to the 'Opening' face. Also, equation (13) summarizes the different types of heat transfer that exist in plasma, where the term (*J*) is the Joule effect energy input [7]:

$$\rho\overrightarrow{Vg}gradh = -div(\vec{q}_{ray}) + div(\bar{\bar{\tau}}.\vec{V}) + \vec{J}_{elect}\vec{E} \tag{13}$$

The effective power supplied to the argon to generate the thermal plasma jet which leads to an increase in the enthalpy and the kinetic energy of the gas as shown by the following relationship (Snabre et al. [7]):

$$P = \rho Q C_P (T_0 - T_a) + \frac{1}{2}\rho Q(U_0^2 - U_a^2) \tag{14}$$

where P, ρ, Q,C_p,T_0,T_a ,U_0 ,U_a are respectively the power delivered to argon, the density of argon at room temperature, the flow rate of argon at room temperature, the specific heat of the argon, the average temperature of the gas at the outlet of the nozzle, the temperature of the gas, the average velocity of the plasma jet at the outlet of the nozzle, the velocity of the gas at the outlet of the nozzle under the conditions of pressure and laboratory temperature.

In this study, a two-dimensional case of a thermal plasma jet was studied using argon as the plasma gas for different powers using the ANSYS-CFX code. The dimensions of the computational domain for the plasma jet are 100 mm and 50 mm for length and height, respectively. The nozzle diameter is 3.0mm, the argon flow rate is 8.4 liters/min, the x-axis is aligned along the inlet, and the y-axis is perpendicular to the x-axis . First, the results of a 2D thermal plasma jet model using the CFX code will be presented in comparison with experimental results (Snabre et al. [7]) for power 790 W. The SST k-ω and RNG k-ε turbulence models were adopted to obtain simulation results. The comparison was made between the results of experimental and numerical simulations. The results presented in Figure 4 show the predicted axial temperature and velocity distributions of the studied argon plasma jet for the different power values.

One can easily conclude that the results obtained (temperature and velocity distributions) by numerical simulations are very close to the experimental results for different power values. For the CFX code, the velocity and temperature profiles calculated using the RNG turbulence model are very close to the experimental results (Snabre et al. [7]) compared to the results obtained using the SST k-ε, the RNG turbulence model gave very accurate results compared to experimental results.

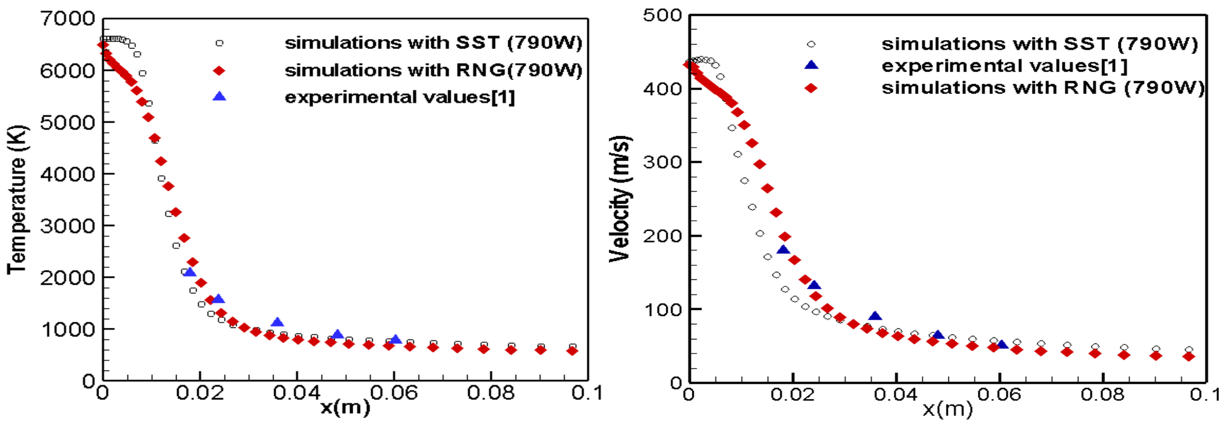

Fig. 4. 2D thermal plasma jet of temperature and velocity results with value of power 790W.

4. RESULTS AND DISCUSSIONS

The k-ε turbulence model has been adopted to obtain concealation results. The dimensions of the substrate calculation domain are respectively 10mm and 50mm for the length and diameter of the cylinder, the substrate material is steel. Speed and temperature profiles are used for three -dimensional mode. The characteristics of the Argon and the Air as a function temperature (density, specific heat, dynamic viscosity and thermal conductivity) were also imposed in the calculation field.

The results presented in figures 5(a) and (b) show the predicted axial temperature and velocity distributions of the argon plasma jet studied for P=1780W for a flow with substrate. For the CFX code, the velocity and temperature profiles obtained using the RNG turbulence model along the central line (x=y=0), take the same shape as those presented in the part dealing with the 2D flow and they are shown in Figure 5 the temperature maximum is within the first millimeter of the nozzle tip, it gradually decreases due to plasma expansion and convection and radiation losses. Also, the temperature contours at the jet inlet are shown in Figures 6(a) and (b), these profiles preserve the appearance of symmetry.

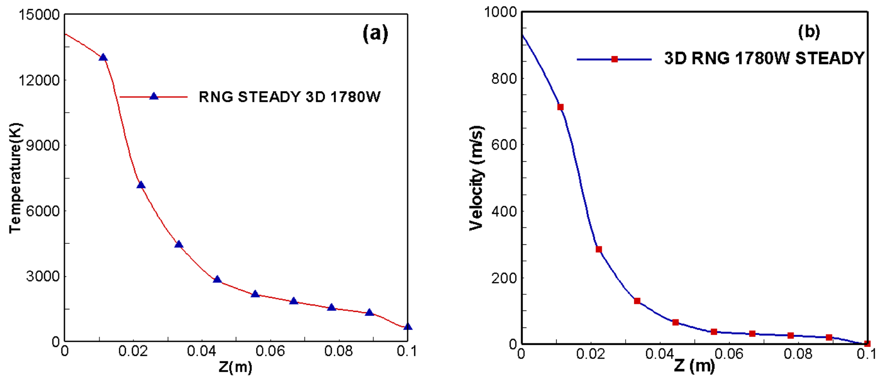

Fig. 5. 3D steady predicted distributions of Temperature and velocity.

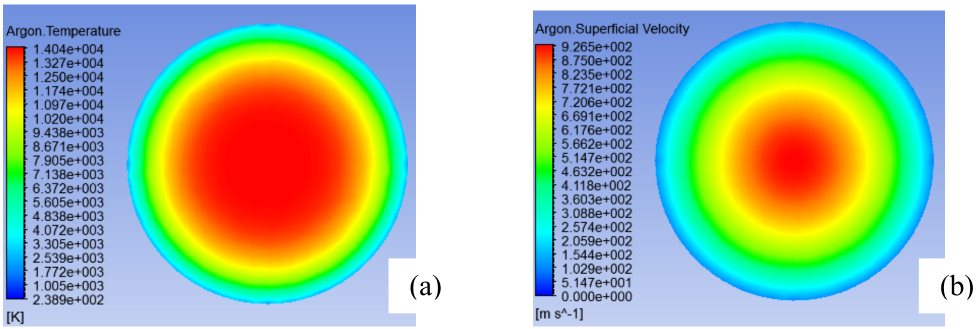

Fig. 6. Inlet distributions for 3D case : (a)Temperature, (b) velocity.

Velocity and temperature contours at the ZY plane level for the substrate less three-dimensional stationary case of an argon jet discharging into air are shown in Figures 7(a) and 7(b). While, the contours of velocities and temperatures at the ZX plane are shown in Figures 8(a) and (b), so Figure 9 shows the air velocity contours on the ZY plane. For all figures 7 to11, the velocity, temperature and volume contours are similar to those obtained for the 2D case.

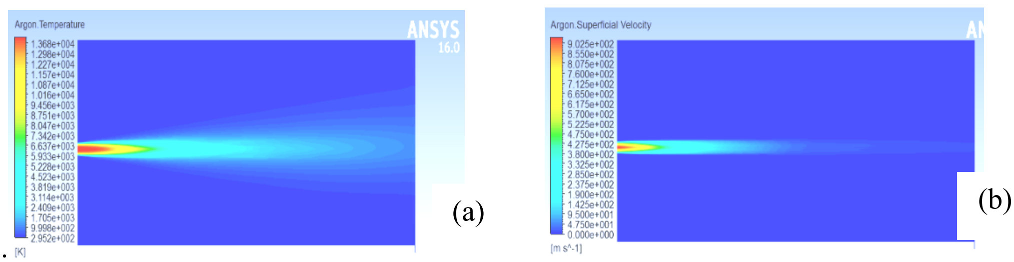

Fig. 7. Argon contours according to ZY plane : (a) for temperature, (b) for velocity.

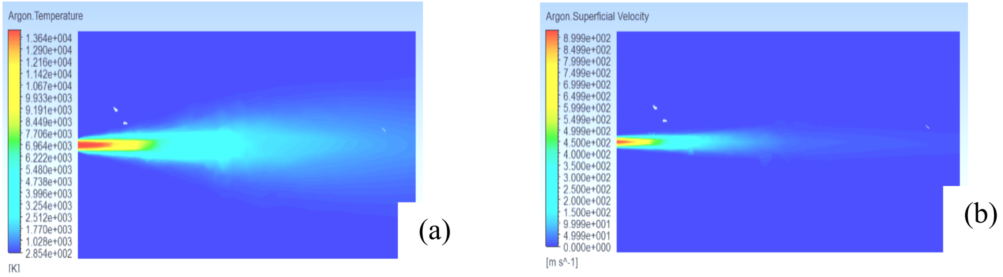

Fig. 8. Argon contours according to XZ plane : (a) for temperature, (b) for velocity.

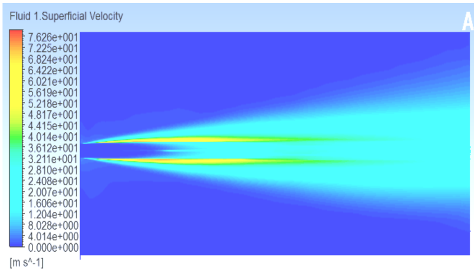

Fig. 9. Air velocity contours according to ZY plane.

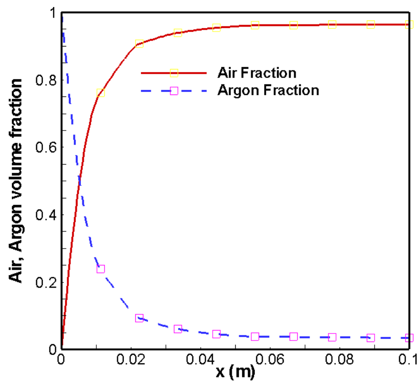

Fig. 10. Air and argon volume fraction distribution according to Z-centraline.

For Figures 11(a) and (b), the substrate temperature contours are globally symmetric, moving away from the Fluid-Solid interface, the substrate temperature decreases at the centerline along the z axis (z=101mm and z=105mm). It also decreases gradually in the direction of x and y by forming isothermal circles.

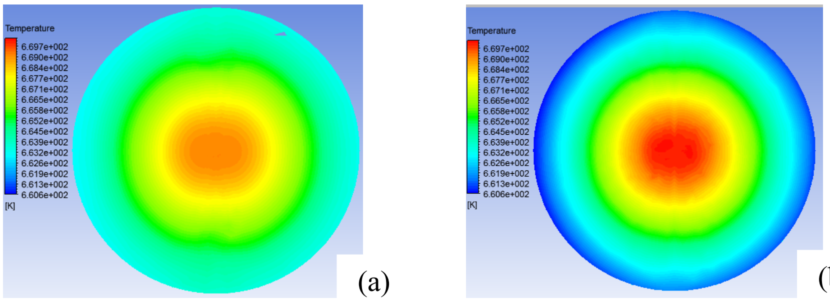

Fig. 11. Substrate temperature contours for 3D case: (a) Temperature for z=101 mm, (b) Temperature for z=105 mm.

Figures 12 and 13 represent the contours of temperatures and velocities of the argon jet and the temperatures of the substrate, these contours are globally symmetrical, the middle line presents the maximum values for each station (for different values of z). It also decreases gradually as it moves away from the torch.

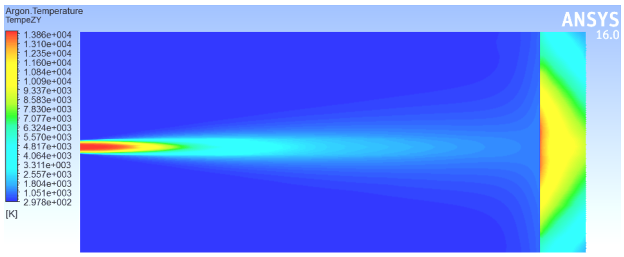

Fig. 12. YZ temperatur argon contours.

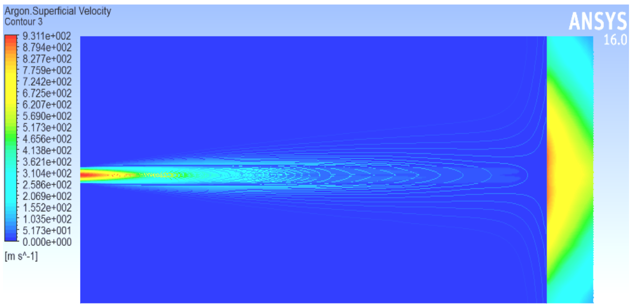

Fig. 13. YZ velocity argon contours

Additively to this, figures 14 and 15 visualize the three-dimensional flow of an argon plasma jet characterized by temperatures and velocities. It was also presented stations for z=0, 25 and 50mm parallel to the inlet face and with the interaction with the substrate.

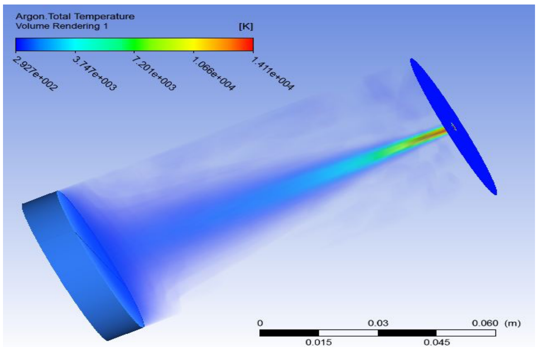

Fig. 14. 3D temperature visualization of plasma jet with substrate interaction

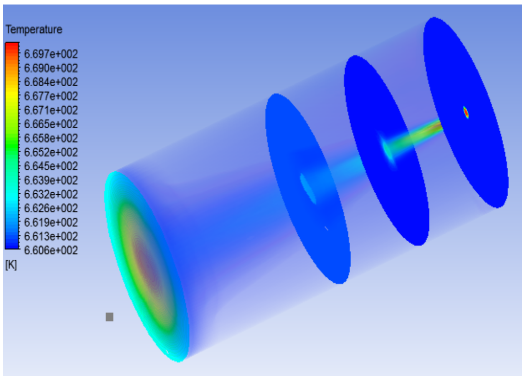

Fig. 15. 3D temperature visualization of plasma jet with substrate interaction and different stations

Finally, the streamlines drawn on figures 17-18 show an abrupt change of direction at the level of the substrate where the velocities Vz are transformed into velocities Vy and Vx (or other components of velocities parallel to the XY plane), this is caused by the impact of the jet on the substrate generating zero or negative Vz velocities in the z direction.

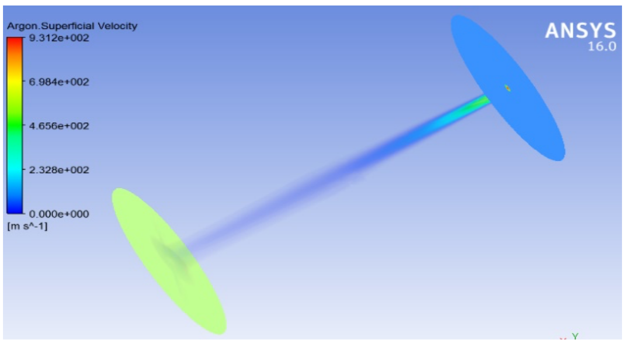

Fig. 16. 3D velocity visualization of plasma jet with substrate interaction.

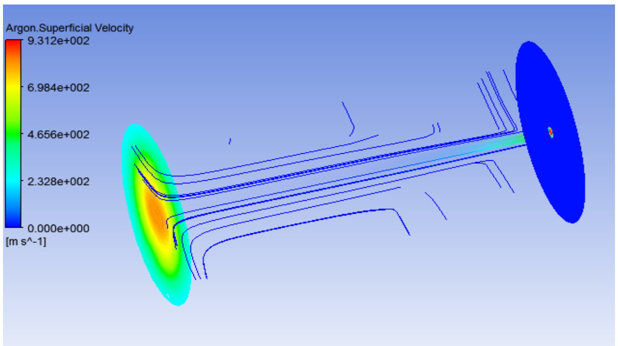

Fig. 17. 3D case for YZ streamlines of plasma jet with substrate interaction.

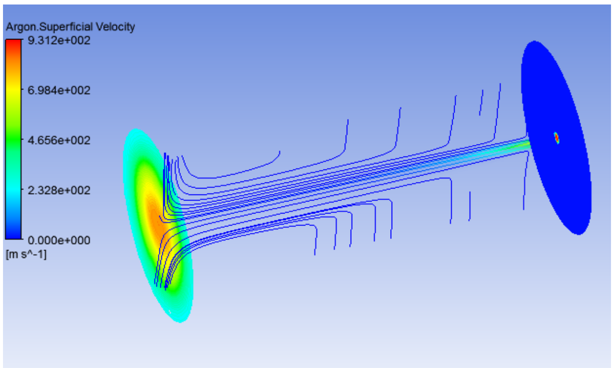

Fig. 18. 3D case for XZ streamlines of plasma jet with substrate interaction.

5. CONCLUSION

Transient two-dimensional simulations in the substrate for the different time values show that the variation of the temperature of the plasma jet is always insignificant near the substrate for any time value (flat curves). The maximum of the temperatures obtained at the level of the substrate in the axial direction (Z axis) are maximum at the interface between the flow and the substrate (i.e. the contact surface at the level of the center line), and the maximum of the temperatures obtained at the level of the substrate in the radial direction (y-axis) are maximum at the center of the substrate (i.e. x=0 and y=0).

On the other hand, and as a second step, a 3D thermal plasma jet discharging in the air was simulated using the ANSYS-CFX code with the RNG k-ε and for the case where the power equals 1780W. The analysis of the turbulent flow was presented for the stationary case, after the convergence of the solution, the results obtained (profile of the velocity and temperature at the entrance) were presented in detailed diagrams and figures. The results obtained by the simulations of a three-dimensional stationary flow are similar to those obtained by the simulations of a two-dimensional stationary flow and the representative curves take the same shape.

As a perspective, we suggest in the future to continue with three-dimensional transient simulations using other turbulence modes and also using, for academic purposes, the data presented in the patent document whose reference is [9] (see appendix attached). This paper suggested using plasma gases. with well-defined percentages and claims that it improves flow characteristics.

REFERENCES

1. Max Ulrich Schoop., 1909. Procédé de production de revêtements métalliques denses, Patent-Nr. 258505, DE.
2. Sarret, F., 2014. Simulation numérique de dépôts céramiques plasma; *doctoral, thesis*, university of Bordeaux, France.
3. Sokolov, D., 2009. Contribution au développement de la projection thermique à très faible pression, doctoral thesis, university of Belfort, France.
4. Boulos, M.I., Fauchais, P and Pfender, E, 1994. Thermal plasmas: Fundamentals and Applications. *Plenum Press*, vol. 1, New York, USA.
5. Baudry, C., 2003. Contribution à la modélisation instationnaire et tridimensionnelle du comportement dynamique de l'arc dans une torche de projection plasma, doctoral thesis, University of Limoges, France.
6. Pfender, E., plasma jet behavior and modeling associated with the plasma spray process, Plasma, Spectroscopy and Software, *Robert-Koch-Strasse 8*, 86343 Koenigsbrunn, Germany, www.plasus.de 29.
7. Snabre, P., Announ, M., Badie, J.M and Granier, B., 1998. Heat transfer around a spherical particle levitated in argon plasma jet, *Eur. Phys. J. AP,* Vol., 3, pp. 287-293.
8. Murphy, A.B., 1995. Transport Coefficients of Air, Argon-Air, Nitrogen-Air, and Oxygen-Air Plasmas, *Plasma Chemistry and Plasma Processing*, 15(2).
9. Nicoud, D et al., 1994. Fascicule de Brevet Europeen, Numéro de dépôt : 91400901.4, 07/12/1994.